AAS 14-449

LONG-TERM DYNAMICS OF FAST ROTATING TETHERS AROUND PLANETARY SATELLITES

Hodei Urrutxua*, Jesús Peláez* and Martin Lara*

We derive a semi-analytic formulation that enables the study of the long-term dynamics of fast-rotating inert tethers around planetary satellites. These equations take into account the coupling between the translational and rotational motion, which has a non-negligible impact on the dynamics, as the orbital motion of the tether center of mass strongly depends on the tether plane of rotation and its spin rate, and vice-versa. We use these governing equations to explore the effects of this coupling on the dynamics, the lifetime of frozen orbits and the precession of the plane of rotation of the tether.

INTRODUCTION

The use of space tethers offers potential advantages to numerous applications in astrodynamics, though many of them still remain unexplored to great extent. Beyond the already known features of inert tethers for orbital maneuvers[1,2] or electrodynamic tethers for active deorbiting,[1,3] just to cite a few, more recent studies have focused in the ability of fast rotating tethers (FRT) to stabilize the orbital dynamics. In this regards, space tethers can be used to stabilize orbits at lagrangian points,[4] or to achieve lower eccentricity and higher inclination *extended* frozen orbits around planetary satellites.[5,6]

Studying frozen orbits and other orbit stability issues requires dealing with the long-term dynamics of a FRT. Its motion can be observed to evolve in various different time scales, such as the self-rotation angular velocity of the tether, $\Omega_\perp$, the orbital angular velocity of the tether center of mass around the planetary satellite, n, the orbital angular velocity of the of the planetary satellite around the planet, n_3, and the long-period time scales in which the orbital elements experience substantial variations in value. The averaging method allows us to get rid of the short-period oscillations of the dynamics, by averaging the equations in the fastest time scales, $\Omega_\perp$, n and n_3, thus yielding equations that govern the long-term variation of the mean orbital elements. Frozen orbits are in fact the stationary solutions for these orbital equations.

For tethers, in general, the translational dynamics of its center of mass, and its rotational dynamics are strongly coupled. We say that a rotating tether is a FRT when $n/\Omega_\perp \ll 1$, in which case, the fact that the tether is rotating allows us to introduce a stroboscopic reference frame for the tether plane of rotation, whose attitude dynamics scales with the ratio $n^2/\Omega_\perp$. Hence, a common assumption for FRTs if that $n/\Omega_\perp \to 0$, which decouples the dynamics, by considering that the tether plane of rotation remains *frozen* in the fast scales. This assumption is perfectly fine for studying the fast dynamics, but becomes invalid for times $n^2\, t/\Omega_\perp \sim \mathcal{O}(1)$. Therefore, the dynamical evolution of the tether plane of rotation also has a long-period time scale in which its attitude changes substantially, and this time scale may be comparable to the time scale in which orbital elements vary. In other words, when one is studying the long-term dynamics of a tethered system, averaging not only the orbital equations but rotational equations too becomes necessary, for consistency, and the problem remains coupled. For instance, as noted in Reference 6 (also shown in Figure 5), frozen orbits computed with a constant orientation of the tether plane of rotation may drastically change over time when one allows the plane of rotation to freely evolve according to its dynamical equations.

*Space Dynamics Group, School of Aeronautical Engineering, Technical University of Madrid (UPM). http://sdg.aero.upm.es/

The current paper is both an extension of Ref. 5 and a natural continuation of Ref. 6. The main part of these derivations is addressed in the Engineering Thesis of Reference 7. The averaged equations for the translational problem were already presented in Ref. 5, though their derivation was only roughly presented, since the point of the paper was not the set of equations but their application to extend frozen orbits. Also, the governing equations for the orbital motion employed in Ref. 6 were derived under the hypothesis of a equatorial configuration of the tether plane of rotation, whereas the alternative formulation introduced in the current paper copes with an arbitrary attitude of the tether given by their Tait-Bryan angles. Additionally, the averaged equations for the rotational problem that are presented in this paper are previously unreleased, so to the authors' knowledge this is the first time that a full formulation for the averaged roto-translational problem is presented, which allows to study the motion of a fast rotating tether around a planetary satellite.

In what follows, we first introduce the concept of a tethered system, describe the dynamics of a rotating tether around a planetary satellite and derive the governing equations of the roto-translational problem. Noticing that its dynamics takes place in different time scales, we apply successively the averaging technique to remove the short period oscillations, so first we derive the roto-translational equations of motion for 'fast' rotating tethers, and then average them again to study the 'long-term' evolution of the system. Finally, we use these governing equations to analyze the effects and consequences of the coupling between the translational and rotational motion, and more particularly how it affects the lifetime of the extended frozen orbits that may be obtained with the use of FRTs,[6] as well as the inherent precession of the tether plane of rotation.

EQUATIONS OF MOTION FOR A ROTATING TETHERS

Translational Motion

Let us consider a tethered system orbiting around a planetary satellite as a particular case of a restricted three-body problem, where without loss of generality we might think of a tether orbiting around the Moon. Figure 2 schematically shows the geometrical layout of the problem. In order to study the orbital motion of the tether center of mass, our dynamical model should take into consideration the following sources of orbital perturbations: 1) the perturbation due to the mutual gravitational interaction of the primary and the tether, 2) the non-uniformity of the primary's gravitational field, and 3) the planet's third body perturbation. In the following, we proceed to detail the modeling of each of these perturbations.

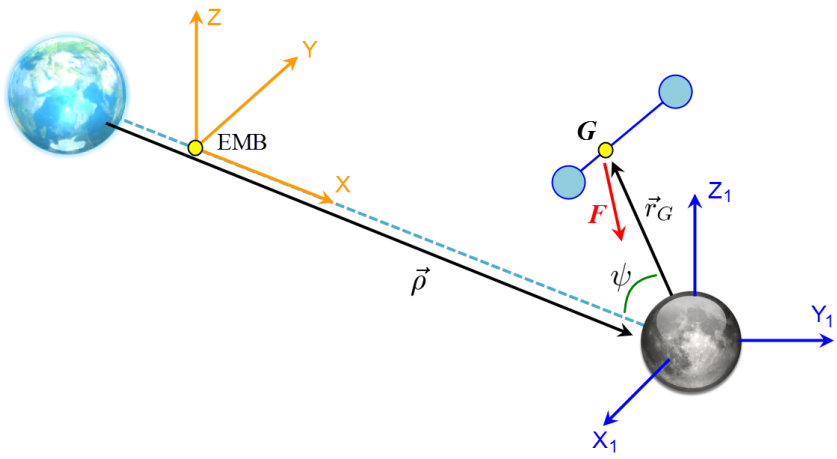

Figure 1: **Illustration of the geometrical layout of the problem under consideration, namely a tether orbiting around a planetary satellite. As an example, the Earth-Moon-Tether system is sketched.**

Because gravity is non-linear, the resultant of the gravitational force on an extensive body does not generally coincide with the force one would obtain by concentrating all the body mass at the system's center of mass. As a result, a non-Keplerian perturbation term arises from the fact that the tether's mass is distributed in a finite volume, which depends solely on the mass geometry and attitude of the tether. The precise orbital

motion of a tether is then studied as a *Full Two-Body* problem, where both bodies, tether and primary, are considered as extensive, i.e. every mass element $\mathrm{d}m$ of the tether is attracted by every $\mathrm{d}M$ of the primary, yielding a double volume integral. The full two-body approach is usually avoided unless it is really necessary, due to the inherent difficulty of the arising expressions, though when one of the two bodies is so slim as a tether, this body could be treated as a linear geometry, reducing one of the volume integrals into a linear integral. Still, this approach implies a heavy mathematical formulation to include increasingly smaller perturbing terms, which is usually avoided by adding further simplifying assumptions, such as neglecting the mutual gravitational coupling between the tether and the primary. Doing so, in order to evaluate the tether perturbation one considers the tether as an extensive body but the primary as a mass point, and reversely, in order to evaluate the perturbation of the non-uniform gravity field of the primary upon the tether, one considers the primary as an extensive body, but the tether as a mass point, thus omitting the mutual gravitational coupling. For simplicity, this is the approach chosen for the current manuscript, though the interested reader may found in References 7 and 8 a detailed derivation of the gravitational actions upon an extensive tether due to a primary with arbitrary number of zonal harmonics, which does include their mutual gravitational coupling.

So, let us consider a tethered system, or by extension simply a tether, formed up by two spacecraft tied one to another by a tether of length L_T, modeled as a long, rigid rod of mass m_T, according to the *extended dumbbell model* approximation. Both spacecraft are modeled as point masses m_1 and m_2 whereas the tether is assumed to have a homogeneous linear mass density $\rho_L = m_T/L_T$. Therefore, the total mass of the tether is $m = m_1 + m_2 + m_T$, and the center of mass of the tethered system, G, is located on the tether itself, somewhere in-between both end-masses, at distances L_1 and L_2 respectively, such that $L_T = L_1 + L_2$, as shown in Figure 2.

In the center of mass of the primary, O, we place a pseudo-inertial coordinate system $\{O; x_1, y_1, z_1\}$, such that the plane $x_1 y_1$ contains the orbital plane of the planetary satellite around the planet and z_1 forms a right-handed frame (see Fig. 1). We define the position vector of the tether's center of mass as $\vec{r}_G = r_G \cdot \vec{u}_G$. Let s be a coordinate indicating the linear position of any differential mass element of the tether, $\mathrm{d}m$, and $\vec{u}$ the unity vector pointing from m_1 to m_2. This allows us to define the angle α as the one formed between the unit vectors $\vec{u}_G$ and $\vec{u}$. Hence, as shown in Figure 2, the position of any $\mathrm{d}m$ of the tether may be expressed as

$$\vec{r} = r_G\,(\vec{u}_G + \eta \cdot \vec{u}),$$

where the more convenient non-dimensional parameter $\eta = s/r_G$ is introduced, such that typically $\eta \ll 1$.

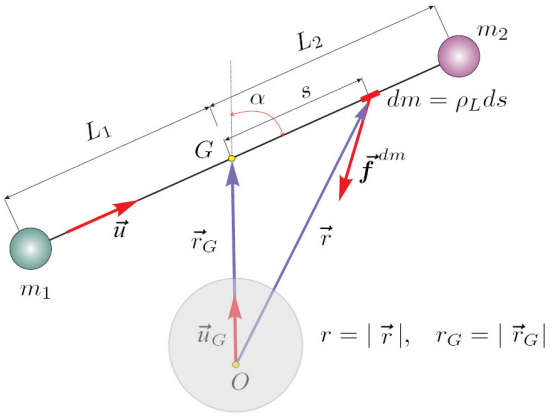

Figure 2: **Scheme showing the rigid tethered system considered in the analysis and the nomenclature used for geometrical variables and vectors in the description of the extended dumbbell model**

Notice that generally the gravitational attraction upon every single mass element $\mathrm{d}m$ of the tether does not need to be aligned with $\vec{u}$, due to the non-uniformity of the primary's gravity field.

Hence, the gravitational potential of a tether, considering the primary as a point mass, is given by

$$V_T = -\frac{\mu}{r_G} \int \frac{\mathrm{d}m}{\sqrt{1 + 2\eta\cos\alpha + \eta^2}}$$

where the integral extends to the whole length of the tether by means of the change of variable $\mathrm{d}m = \rho_L\, r_G\, \mathrm{d}\eta$. Developing the above integral in Legendre polynomials leads to

$$V_T = -\frac{\mu\, m}{r_G} - \frac{\mu\, m}{r_G} \sum_{n=2}^{\infty} (-1)^n \left(\frac{L_T}{r_G}\right)^n a_n\, P_n(\cos\alpha)$$

where α is the angle formed between unit vectors $\vec{u}_G$ and $\vec{u}$, and the non-dimensioal coefficients a_n are known functions of the mass geometry of the tether. Further detail on this derivation and values of the functions a_n may be found in References 4, 7 and 8.

Retaining up to second order terms in the small parameter L_T/r_G, and omitting the zeroth order term of the potential yields the disturbing function of the gravitational perturbation of the tether, $\mathcal{R}_T$, given by

$$\mathcal{R}_T = -\frac{\mu\, m}{r_G}\left[\frac{L_T^2}{r_G^2}\, a_2\, P_2(\vec{u}_G \cdot \vec{u}) + \mathcal{O}\left(\frac{L_T}{r_G}\right)^3\right] \tag{1}$$

with

$$a_2 = \left(1 - \frac{m_1}{m} - \frac{1}{2}\,\frac{m_T}{m}\right)\left(\frac{m_1}{m} + \frac{1}{2}\,\frac{m_T}{m}\right) - \frac{1}{6}\,\frac{m_T}{m}.$$

In the most general case, $0 < a_2 < 1/4$. However, it can be easily shown that, for equal end masses, $1/12 < a_2 < 1/4$, where the highest value, $a_2 = 1/4$, corresponds to a tether of negligible mass, $m_T = 0$, and the other extreme value, $a_2 = 1/12$, corresponds to $m_T = m$.

The next orbital perturbation to be considered is the non-uniformity of the primary's gravitational field, which is very conveniently expressed by its expansion in spherical harmonics. Although a general representation of the gravity field requires zonal, sectorial and tesseral harmonics, it can be proven that the latter two average out when studying the long-term dynamics, i.e. averaging the orbital motion around the primary. Therefore, for the current study suffices to consider only the zonal harmonics of the primary. The disturbing potential $\mathcal{R}_{Jn}$ due to the gravitational perturbation of the J_l zonal harmonics of the primary is given by

$$\mathcal{R}_{Jn} = -\frac{\mu\, m}{r_G}\sum_{n=2}^{\infty}\left(\frac{R}{r_G}\right)^n J_n\, P_n(\vec{u}_G \cdot \vec{k}_1) \tag{2}$$

where $\vec{k}_1$ is a unit vector aligned with the primary's pole, which coincides with the z_1 axis, and R is a reference radius. Very often the oblateness of the primary is the main contribution to the non-uniformity of its gravity field and J_2 is several orders of magnitude larger than any other zonal harmonic. This taken into consideration, we find adequate to retain just terms up to second order in the small parameter R/r_G, in order to keep our analytical derivations clear, knowing that further zonals may be easily added later on. Thus, the perturbing potential due to the oblateness of the primary, $\mathcal{R}_{J2}$, yields

$$\mathcal{R}_{J2} = \frac{\mu\, m}{r_G}\left[\frac{R^2}{r_G^2}\, J_2\, P_2(\vec{u}_G \cdot \vec{k}_1) + \mathcal{O}\left(\frac{R}{r_G}\right)^3\right]. \tag{3}$$

Note the striking analogy between the oblateness perturbation, $\mathcal{R}_{J2}$, and the non-Keplerian perturbation of the tether, $\mathcal{R}_T$. If the tether length is in the direction of $\vec{k}$, then the orbital acceleration due to the tether physical length directly substracts to the acceleration caused by the oblateness of the central body. Therefore, if we were able to maintain a non-rotating tether with this constant orientation along its orbital motion, then we would have an artificial way of varying the apparent oblateness of a natural body, though it seems unlikely that the tether would evolve in this special configuration without active control.[6]

Finally, we also need to include in our model the third-body perturbation of the planet. The disturbing potential of the third-body perturbation, $\mathcal{R}_{3B}$, can be expressed by the series expansion

$$\mathcal{R}_{3B} = -\frac{\mu_3\, m}{\rho}\sum_{n=2}^{\infty}\left(\frac{r_G}{\rho}\right)^n P_n(\cos\psi),$$

where μ_3 is the gravitational parameter of the planet, ρ is the distance from the satellite to the planet and ψ is the angle formed between the position vector of the tether center of mass, $\vec{r}_G$, and the position vector of

planet, $\vec{\rho}$ (see Figure 1). For consistency, we may as well retain only the first term in the summation and neglect the rest, so that the third-body disturbing potential reduces to

$$\mathcal{R}_{3B} = -\frac{\mu_3\, m}{\rho}\left[\frac{r_G^2}{\rho^2}\, P_2(\cos\psi) + \mathcal{O}\left(\frac{r_G}{\rho}\right)^3\right]. \tag{4}$$

Now, the total disturbing potential, $\mathcal{R}$, will be the sum of the three contributions just presented, namely

$$\mathcal{R} = \mathcal{R}_T + \mathcal{R}_{J2} + \mathcal{R}_{3B},$$

so substituting equations (1), (3) and (4), the total disturbing potential takes the form

$$\mathcal{R} = -\frac{\mu\, m}{r_G^3}\left[L_T^2\, a_2\, P_2(\vec{u}_G\cdot\vec{u}) - R^2\, J_2\, P_2(\vec{u}_G\cdot\vec{k}_1)\right] - \frac{\mu_3\, m}{\rho^3}\, r_G^2\, P_2(\cos\psi). \tag{5}$$

Once the disturbing potential is known, the orbital motion of the tether around the primary may be studied using the Lagrange planetary equations, which provide the time evolution of the orbital elements

$$\frac{\mathrm{d}a}{\mathrm{d}t} = \frac{2}{m\,n\,a}\,\frac{\partial\mathcal{R}}{\partial M_0} \tag{6}$$

$$\frac{\mathrm{d}e}{\mathrm{d}t} = \frac{1-e^2}{m\,n\,a^2\,e}\,\frac{\partial\mathcal{R}}{\partial M_0} + \frac{\sqrt{1-e^2}}{m\,n\,a^2\,e}\,\frac{\partial\mathcal{R}}{\partial\omega} \tag{7}$$

$$\frac{\mathrm{d}i}{\mathrm{d}t} = \frac{1}{m\,n\,a^2\,\sqrt{1-e^2}\,\sin i}\left[\frac{\partial\mathcal{R}}{\partial\Omega} - \cos i\,\frac{\partial\mathcal{R}}{\partial\omega}\right] \tag{8}$$

$$\frac{\mathrm{d}\omega}{\mathrm{d}t} = -\frac{\sqrt{1-e^2}}{m\,n\,a^2\,e}\,\frac{\partial\mathcal{R}}{\partial e} + \frac{\cot i}{m\,n\,a^2\,\sqrt{1-e^2}}\,\frac{\partial\mathcal{R}}{\partial i} \tag{9}$$

$$\frac{\mathrm{d}\Omega}{\mathrm{d}t} = \frac{-1}{m\,n\,a^2\,\sqrt{1-e^2}\,\sin i}\,\frac{\partial\mathcal{R}}{\partial i} \tag{10}$$

$$\frac{\mathrm{d}M}{\mathrm{d}t} = n - \frac{1-e^2}{m\,n\,a^2\,e}\,\frac{\partial\mathcal{R}}{\partial e} - \frac{2}{m\,n\,a}\,\frac{\partial\mathcal{R}}{\partial a} \tag{11}$$

where $\{a, e, i, \omega, \Omega, M\}$ are the classical orbital elements and $n = \sqrt{\mu/a^3}$ is the mean orbital motion around the primary.

Rotational Motion

The attitude dynamics of the tether is described by the time evolution of the angular momentum vector at its center of mass, $\vec{H}_G$. Then, the rotational motion is governed by the vector equation

$$\frac{\mathrm{d}\vec{H}_G}{\mathrm{d}t} = \vec{M}$$

where $\vec{M}$ is the torque produced by the external forces upon the tether. Thus, $\vec{M}$ is basically the gravity gradient upon the tethered system. Neglecting the mutual gravitational coupling between the tether and the primary (i.e. assuming an extensive tether but a mass-point primary), as well as the gravity torque due to the presence of the third-body, the torque is obtained from the evaluation of the integral

$$\vec{M} = -\frac{\mu}{r_G}\,\vec{u}\wedge\vec{u}_G\int_m \frac{\eta\,\mathrm{d}m}{(\sqrt{1+2\,\eta\,\cos\alpha+\eta^2})^3},$$

where the integral extends to the whole length of the tether. After expanding the denominator in power series of η, and retaining just the first term of the expansion, the gravitational torque is given by the expression[8]

$$\vec{M} = \frac{\mu\, m}{r_G}(\vec{u}\wedge\vec{u_G})\left[3\,a_2\,\frac{L_T^2}{r_G^2}\,(\vec{u}_G\cdot\vec{u}) + \mathcal{O}\left(\frac{L_T}{r_G}\right)^3\right]. \tag{12}$$

In the system defined by the axes of maxima inertia, there is a null moment of inertia around $\vec{u}$, and the inertia tensor at the tether center of mass, $\bar{\bar{I}}_G$, is

$$\bar{\bar{I}}_G = \begin{pmatrix} 0 & 0 & 0 \\ 0 & \mathcal{I} & 0 \\ 0 & 0 & \mathcal{I} \end{pmatrix}$$

where $\mathcal{I} = m\, a_2\, L_T^2$. Then, knowing the angular velocity of the tether, $\vec{\Omega}$, is given by

$$\vec{\Omega} = \vec{u} \wedge \frac{\mathrm{d}\vec{u}}{\mathrm{d}t} + (\vec{u} \cdot \vec{\Omega})\, \vec{u},$$

the angular momentum $\vec{H}_G$ can be written as

$$\vec{H}_G = \bar{\bar{I}}_G \circ \vec{\Omega} = \mathcal{I}\, \vec{u} \wedge (\vec{\Omega} \wedge \vec{u}) = \mathcal{I}\, \vec{u} \wedge \frac{\mathrm{d}\vec{u}}{\mathrm{d}t}.$$

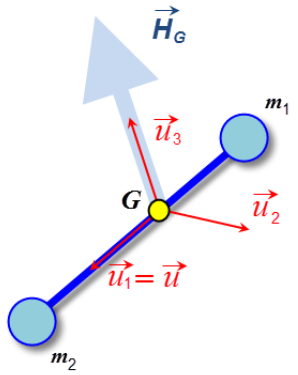

Figure 3: Tether body-fixed reference frame and angular momentum vector, $\vec{H}_G$

The angular momentum turns out to be normal to the tether, which suggests using a body-fixed reference system $\{G; \vec{u}_1, \vec{u}_2, \vec{u}_3\}$ (see Figure 3), where the unit vectors defining the reference frame are

$$\vec{u}_1 = \vec{u}, \qquad \vec{u}_2 = \frac{\mathrm{d}\vec{u}/\mathrm{d}t}{|\,\mathrm{d}\vec{u}/\mathrm{d}t|}, \qquad \vec{u}_3 = \vec{u}_1 \wedge \vec{u}_2$$

Thus, the angular momentum may be rewritten as

$$\vec{H}_G = \mathcal{I}\, \Omega_\perp \vec{u}_3, \quad \text{where} \quad \Omega_\perp = |\vec{u} \wedge \mathrm{d}\vec{u}/\mathrm{d}t| = |\,\mathrm{d}\vec{u}/\mathrm{d}t|$$

so the angular momentum equation may then be expressed as

$$\frac{\mathrm{d}\vec{H}_G}{\mathrm{d}t} = \mathcal{I} \left(\frac{\mathrm{d}\Omega_\perp}{\mathrm{d}t}\, \vec{u}_3 + \Omega_\perp \frac{\mathrm{d}\vec{u}_3}{\mathrm{d}t} \right).$$

Taking the dot product of the later equation with $\vec{u}_3$, and taking twice the cross product with $\vec{u}_3$ leads to the equations

$$\frac{\mathrm{d}\Omega_\perp}{\mathrm{d}t} = \frac{\vec{M} \cdot \vec{u}_3}{\mathcal{I}}$$
$$\frac{\mathrm{d}\vec{u}_3}{\mathrm{d}t} = \frac{\vec{M} \cdot \vec{u}_2}{\Omega_\perp \mathcal{I}}\, \vec{u}_2$$

that along with the orthogonality relation $\vec{u}_2 = \vec{u}_3 \wedge \vec{u}_1$ and the evolution equation for the unit vector $\vec{u}_1$

$$\frac{\mathrm{d}\vec{u}_1}{\mathrm{d}t} = \vec{\Omega} \wedge \vec{u}_1 = \Omega_\perp \vec{u}_2$$

completely define the rotational dynamics of the tether. Furthermore, the constraints $|\vec{u}_1| = |\vec{u}_3| = 1$ and $\vec{u}_1 \cdot \vec{u}_3 = 0$ reduce the dimension of the system to a set of only four differential equations.

In order to describe the rotational state of the tether in a more convenient manner, we introduce a set of *Tait-Bryan* angles, $\{\phi_1, \phi_2, \phi_3\}$, in the sequence XYZ. Then, the body-fixed frame, $\{\vec{u}_1, \vec{u}_2, \vec{u}_3\}$, may be

related to the inertial frame, $\{\vec{\imath}_1, \vec{\jmath}_1, \vec{k}_1\}$, by means of the following relations

$$\begin{aligned}\vec{u}_1 = & \quad (\cos\phi_2\ \cos\phi_3)\,\vec{\imath}_1 \\ & + (\cos\phi_1\ \sin\phi_3 + \sin\phi_1\ \sin\phi_2\ \cos\phi_3)\,\vec{\jmath}_1 \\ & + (\sin\phi_1\ \sin\phi_3 - \cos\phi_1\ \sin\phi_2\ \cos\phi_3)\,\vec{k}_1\end{aligned} \tag{13}$$

$$\begin{aligned}\vec{u}_2 = & -(\cos\phi_2\ \sin\phi_3)\,\vec{\imath}_1 \\ & + (\cos\phi_1\ \cos\phi_3 - \sin\phi_1\ \sin\phi_2\ \sin\phi_3)\,\vec{\jmath}_1 \\ & + (\sin\phi_1\ \cos\phi_3 + \cos\phi_1\ \sin\phi_2\ \sin\phi_3)\,\vec{k}_1\end{aligned} \tag{14}$$

$$\begin{aligned}\vec{u}_3 = & \quad (\sin\phi_2)\,\vec{\imath}_1 \\ & - (\sin\phi_1\ \cos\phi_2)\,\vec{\jmath}_1 \\ & + (\cos\phi_1\ \cos\phi_2)\,\vec{k}_1\end{aligned} \tag{15}$$

Hence, after some algebra we finally get that attitude dynamics of a rotating tether is governed by this set of four scalar differential equations[4,6]

$$\frac{\mathrm{d}\phi_1}{\mathrm{d}t} = -\frac{\vec{M}\cdot\vec{u}_2}{\Omega_\perp\,\mathcal{I}}\,\frac{\cos\phi_3}{\cos\phi_2} \tag{16}$$

$$\frac{\mathrm{d}\phi_2}{\mathrm{d}t} = -\frac{\vec{M}\cdot\vec{u}_2}{\Omega_\perp\,\mathcal{I}}\,\sin\phi_3 \tag{17}$$

$$\frac{\mathrm{d}\phi_3}{\mathrm{d}t} = \Omega_\perp + \frac{\vec{M}\cdot\vec{u}_2}{\Omega_\perp\,\mathcal{I}}\,\cos\phi_3\,\tan\phi_2 \tag{18}$$

$$\frac{\mathrm{d}\Omega_\perp}{\mathrm{d}t} = \frac{\vec{M}\cdot\vec{u}_3}{\mathcal{I}} \tag{19}$$

Additionally, if (p, q, r) are the components of the angular velocity $\vec{\Omega}$ in the tether body-fixed frame, these components can be expressed in terms of the time derivatives of the Tait-Bryan angles through the following relations

$$p = \dot{\phi}_2\,\sin\phi_3 + \dot{\phi}_1\,\cos\phi_2\,\cos\phi_3 \tag{20}$$

$$q = \dot{\phi}_2\,\cos\phi_3 - \dot{\phi}_1\,\cos\phi_2\,\sin\phi_3 \tag{21}$$

$$r = \dot{\phi}_3 + \dot{\phi}_1\,\sin\phi_2 \tag{22}$$

EQUATIONS OF MOTION FOR 'FAST' ROTATING TETHERS

A close look at Eqs. (16) to (19) reveals that for a rotating tether there are several different time scales involved in the description of its dynamics. It is important to know about these scales, as they represent, so to say, the real nature of the motion. Different aspects of the motion of the tether are associated to one or another time scale enclosed in the problem. Usually the shortest time scale is the one related to the spinning of the tether, $\Omega_\perp$. The characteristic time of the tether's rotation is then $T_1 = 1/\Omega_\perp$. This allow us to introduce the non-dimensional time τ_1 as

$$\tau_1 = t/T_1 = \Omega_\perp\,t.$$

Another time scale of the problem, usually much larger than the prior, is that associated to the orbital motion of the tether, whose characteristic time is $T_2 = 1/n$, where n stands for the mean orbital motion. Thus, we can introduce yet another non-dimensional time,

$$\tau_2 = t/T_2 = n\,t.$$

When for a rotating tether the relation $\Omega_\perp/n \gg 1$ is satisfied, we refer to it a *fast* rotating tether (FRT). In that case, the two time scales turn out to be clearly differentiated, since their characteristic times fulfill the relation $T_1/T_2 \ll 1$. Hence, in the time scale of the orbital period, where $\tau_2 \sim \mathcal{O}(1)$, the fast rotating tether has given several turns around the angular momentum vector, $\vec{H}_G$. Oppositely, in the time scale of the self-rotation of the tether, i.e. for $\tau_1 \sim \mathcal{O}(1)$, the evolution of the angular variables whose changing rate depends on τ_2, barely suffer any variations; thus, they could be treated as *frozen* variables when studying the motion in the *fast* time scale, and in this time scale the angular momentum vector remains constant in the inertial space. To stress out the later point, we may rewrite equations (16) to (19) in terms of the non-dimensional time τ_1, which after substituting the torque from Eq. (12) leads to

$$\frac{\mathrm{d}\phi_1}{\mathrm{d}\tau_1} = \mathcal{O}\left(\frac{n}{\Omega_\perp}\right)^2 \qquad \frac{\mathrm{d}\phi_2}{\mathrm{d}\tau_1} = \mathcal{O}\left(\frac{n}{\Omega_\perp}\right)^2 \qquad \frac{\mathrm{d}\phi_3}{\mathrm{d}\tau_1} = 1 + \mathcal{O}\left(\frac{n}{\Omega_\perp}\right)^2 \qquad \frac{\mathrm{d}\Omega_\perp}{\mathrm{d}\tau_1} = \mathcal{O}\left(\frac{n^2}{\Omega_\perp}\right)$$

Averaging over the Rotation of the Tether

Then, we can clearly observe that the angle $\phi_3 \approx \tau_1$ is a *fast* variable that evolves in the *fast* time scale, while ϕ_1, ϕ_2 and $\Omega_\perp$ are *slow* variables that evolve in a larger time scale. This fact is very meaningful, for it brings the possibility of using the averaging method to find the time evolution of the system in the slower time scale, $\tau_2 \sim \mathcal{O}(1)$, while getting rid of the short period oscillations associated to the fast time scale. Then, if

$$\frac{\mathrm{d}\Phi}{\mathrm{d}\tau_1} = f\left(\phi_1, \phi_2, \phi_3, \Omega_\perp\right)$$

is a generic form for any of the equations (16) to (19), the corresponding *averaged* equation would take the form

$$\left\langle \frac{\mathrm{d}\Phi}{\mathrm{d}\tau_1} \right\rangle = \frac{1}{2\,\pi} \int_0^{2\pi} f\left(\phi_1, \phi_2, \phi_3, \Omega_\perp\right)\, \mathrm{d}\tau_1$$

where ϕ_1, ϕ_2 and $\Omega_\perp$ are handled as constant variables in the integration, and $\phi_3 \approx \tau_1 + \phi_{30}$.

To efficiently perform an averaging on the fast variable ϕ_3 it is convenient to introduce a *stroboscopic* reference frame, $\{G; \vec{v}_1, \vec{v}_2, \vec{v}_3\}$, that relates to the body-fixed reference frame through

$$\begin{aligned}
\vec{u}_1 &= +\cos\phi_3\, \vec{v}_1 + \sin\phi_3\, \vec{v}_2 \\
\vec{u}_2 &= -\sin\phi_3\, \vec{v}_1 + \cos\phi_3\, \vec{v}_2 \\
\vec{u}_3 &= \vec{v}_3
\end{aligned}$$

For a FRT, the stroboscopic frame is attached to the real plane where the tether is rotating, so that $\vec{v}_1$ and $\vec{v}_2$ define the plane of rotation of the tether. The stroboscopic frame evolves in a slow time scale, since $\vec{v}_1$ and $\vec{v}_2$ do not depend on ϕ_3, and remains nearly constant in the fast time scale, $\tau_1 \sim \mathcal{O}(1)$.

Regarding the averaging process, we realize that the only dependence with the fast variable ϕ_3 appears implicitly through the unit vectors $\vec{u}_1$ and $\vec{u}_2$, and hence through the angle α as well, given by

$$\cos\alpha = \vec{u}_G \cdot \vec{u}_1 = \cos\phi_3\, (\vec{u}_G \cdot \vec{v}_1) + \sin\phi_3\, (\vec{u}_G \cdot \vec{v}_2)$$

while every other variable is to be considered as a constant in the averaging process. All of the expressions we will have to average can be reduced, in the last extend, to any of the following elemental combinations of α and ϕ_3

$$\langle \cos\phi_3 \rangle = \langle \sin\phi_3 \rangle = \langle \sin\phi_3 \cdot \cos\phi_3 \rangle = \langle \cos^2\phi_3 \cdot \sin\phi_3 \rangle = \langle \cos\phi_3 \cdot \sin^2\phi_3 \rangle = 0$$

$$\langle \cos\alpha \rangle = \langle \cos^2\alpha \cdot \cos\phi_3 \rangle = \langle \cos^2\alpha \cdot \sin\phi_3 \rangle = 0$$

$$\langle \cos^2\alpha \rangle = \frac{1}{2}\,(\vec{u}_G \cdot \vec{v}_1)^2 + \frac{1}{2}\,(\vec{u}_G \cdot \vec{v}_2)^2$$

$$\langle \cos^2 \phi_3 \rangle = \frac{1}{2} \qquad \langle \cos\alpha \cdot \cos\phi_3 \rangle = \frac{1}{2} (\vec{u}_G \cdot \vec{v}_1)$$
$$\langle \sin^2 \phi_3 \rangle = \frac{1}{2} \qquad \langle \cos\alpha \cdot \sin\phi_3 \rangle = \frac{1}{2} (\vec{u}_G \cdot \vec{v}_2)$$

Translational Problem

The orbital motion of the tether does not depend on ϕ_3 except through the perturbing potential, $\mathcal{R}$. Taking the last relations into account, averaging the disturbing potential is straightforward, since the third-body potential, $\mathcal{R}_{3B}$ and the potential due to the J_2 perturbation, $\mathcal{R}_{J2}$, both remains unchanged. However, $\mathcal{R}_T$ must be averaged since $\cos\alpha$ depends on ϕ_3. Thus, the averaged perturbing potentials, indicated with a tilde marker, turn into

$$\tilde{\mathcal{R}}_T = + \frac{\mu\, m}{r_G^3}\, a_2\, L_T^2 \left[\frac{1}{2} - \frac{3}{4} (\vec{v}_1 \cdot \vec{u}_G)^2 - \frac{3}{4} (\vec{v}_2 \cdot \vec{u}_G)^2 \right] \tag{23}$$
$$\tilde{\mathcal{R}}_{J2} = + \frac{\mu\, m}{r_G^3}\, J_2\, R^2 P_2(\vec{u}_G \cdot \vec{k}) \tag{24}$$
$$\tilde{\mathcal{R}}_{3B} = - \frac{\mu\, m}{\rho^3}\, r_G^2\, P_2(\cos\psi) \tag{25}$$

Rotational Problem

Proceeding similarly for the attitude dynamics, and using the vector relationship $(\vec{u}_1 \wedge \vec{u}_G) \cdot \vec{u}_2 = -\vec{u}_G \cdot \vec{u}_3$, we average equations (16) to (19), which finally yields

$$\frac{\mathrm{d}\phi_1}{\mathrm{d}t} = \frac{3\,\mu}{2\,\Omega_\perp} \frac{1}{\cos\phi_2} \frac{1}{r_G^3} (\vec{u}_G \cdot \vec{v}_1) (\vec{u}_G \cdot \vec{v}_3) \tag{26}$$
$$\frac{\mathrm{d}\phi_2}{\mathrm{d}t} = \frac{3\,\mu}{2\,\Omega_\perp} \frac{1}{r_G^3} (\vec{u}_G \cdot \vec{v}_2) (\vec{u}_G \cdot \vec{v}_3) \tag{27}$$
$$\frac{\mathrm{d}\phi_3}{\mathrm{d}t} = \Omega_\perp - \frac{3\,\mu}{2\,\Omega_\perp} \tan\phi_2 \frac{1}{r_G^3} (\vec{u}_G \cdot \vec{v}_1) (\vec{u}_G \cdot \vec{v}_3) \tag{28}$$
$$\frac{\mathrm{d}\Omega_\perp}{\mathrm{d}t} = 0 \tag{29}$$

where the angles $\{\phi_1, \phi_2, \phi_3\}$ now represent the *mean* values of the attitude of the tether, and are valid for time scales $t \gg T_1$.

If we study now the averaged rotational dynamics given by Eqs. (26) to (29), but in the slow time scale, $\tau_2 \sim \mathcal{O}(1)$, the rotational problem becomes

$$\frac{\mathrm{d}\phi_1}{\mathrm{d}\tau_2} = \mathcal{O}\left(\frac{n}{\Omega_\perp}\right) \qquad \frac{\mathrm{d}\phi_2}{\mathrm{d}\tau_2} = \mathcal{O}\left(\frac{n}{\Omega_\perp}\right) \qquad \frac{\mathrm{d}\phi_3}{\mathrm{d}\tau_2} = \left(\frac{\Omega_\perp}{n}\right) - \mathcal{O}\left(\frac{n}{\Omega_\perp}\right) \qquad \frac{\mathrm{d}\Omega_\perp}{\mathrm{d}\tau_2} = 0$$

As $n \ll \Omega_\perp$ for a FRT, we get the asymptotic solution $\dot{\phi}_1 = \dot{\phi}_2 = 0$ in the limit $n/\Omega_\perp \to 0$, and the orientation of the tether plane of rotation remains constant in time. This fact is of great relevance, since it implies that rotational and translational motions decouple. This simplification is done very often, yet the neglected effects imply that the FRT's angular momentum will actually slowly precess, at a rate that depends on the ratio of the orbital mean motion to the FRT's self rotation speed. If uncontrolled, this small precession will have a non-negligible impact in the long-term dynamical state of the system, as we shall see in the next sections. However, the rise of this precession may be delayed simply by increasing the tether's rotation, $\Omega_\perp$, or even canceled by applying small control torques, which given the considerable length of space tethers results in a fairly inexpensive control mechanism.

Averaging over the Orbital Motion

As we pointed out in the preceding section and used for our advantage, the dynamics of a FRT evolve in many different time scales, encouraging us to exploit the averaging technique to mask the short period oscillations and focus on the long-term dynamical effects. So far we have identified two main time scales, namely the time scale associated to the self-rotation of the tether, with characteristic time $T_1 = 1/\Omega_\perp$, and the slower time scale in which the tether revolves around the planetary satellite, with a characteristic time $T_2 = 1/n$. However, this is just the top of the iceberg, and even slower time scales may be identified.

For instance, one of the perturbations considered is the third-body perturbation of the planet, whose motions takes places in the time scales in which the satellite revolves around the planet. This scale allows us to introduce a new characteristic time, $T_3 = 1/n_3$, where $n_3 = \sqrt{\mu_3/a_{3B}^3}$ is the mean orbital motion of the satellites around the planet, and a_{3B} stands for the semi-major axis of its orbit. Thus we can introduce the non-dimensional time

$$\tau_3 = t/T_3 = n_3\, t$$

and for the case of most planetary satellites in the Solar System, we observe that $n/n_3 \gg 1$.

Beyond this, we still find the characteristic time in which the tether's orbit evolves, T, which represents the time scale where the tether's long-term motion occurs and its orbital elements vary noticeably. Therefore, we may introduce the new non-dimensional time $\tau = t/T$. The latter is the time scale where frozen orbits become meaningful. The variation of most orbital elements is actually a slow process that takes place along many orbital revolutions around the primary body. Attending at the unperturbed Lagrange planetary equations, Eqs. (6-11), and reformulating them in the time scale $\tau_2 \sim \mathcal{O}(1)$, we clearly see that

$$\frac{\mathrm{d}a}{\mathrm{d}\tau_2} \simeq \frac{\mathrm{d}e}{\mathrm{d}\tau_2} \simeq \frac{\mathrm{d}i}{\mathrm{d}\tau_2} \simeq \frac{\mathrm{d}\Omega}{\mathrm{d}\tau_2} \simeq \frac{\mathrm{d}\omega}{\mathrm{d}\tau_2} = \mathcal{O}\left(\frac{1}{n}\right)^2 \qquad \text{but} \qquad \frac{\mathrm{d}M}{\mathrm{d}\tau_2} \sim 1 + \mathcal{O}\left(\frac{1}{n}\right)^2$$

meaning that in the natural scale in which the anomaly varies, the rest of elements remain frozen, since they vary in the time scale $\tau = \mathcal{O}(1)$. Thus, now τ_1, τ_2 and τ_3 are all going to be fast variables compared to τ, i.e.

$$\tau \ll \tau_3 \ll \tau_2 \ll \tau_1$$

whereas their associated characteristic times fulfill the inverse relations

$$T \gg T_3 \gg T_2 \gg T_1$$

For the sake of example, we may consider a FRT orbiting around the Moon. For this case, a typical rotation speed for FRT is on the order of a minute, whereas a typical orbital period for a Moon orbiter is on the order of the hour, the Moon takes nearly one month to revolve around the Earth, and the long-term variations of the orbital elements of a Moon orbiter may take as long the whole mission lifetime.

Hence, if we aim the focus on the long-term dynamics of the system, we require equations of motion that adequately keep track of the secular and long-period effects, while getting rid of the short-period oscillations taking place in each and every of the faster time scales cited above. For this purpose we shall take advantage again of the averaging technique and apply it successively to the newly identified fast-evolving variables in our problem.

The averaging of a magnitude Q is really done in the time along a period, so if we wish to use another integration variable rather than time, it is neccessary that it changes linearly with time, as in the case of the mean anomaly, M. However, expressing the perturbing potentials as functions of orbital elements is more easily accomplished by using the true anomaly, ν, through the relations

$$r_G = \frac{a\,(1-e^2)}{1 + e\,\cos\nu}$$

and

$$\begin{aligned}\vec{u}_G = \;& [\cos(\Omega)\,\cos(\omega+\nu) - \cos(i)\,\sin(\Omega)\,\sin(\omega+\nu)]\,\vec{\imath} + \\ & + [\sin(\Omega)\,\cos(\omega+\nu) + \cos(i)\,\cos(\Omega)\,\sin(\omega+\nu)]\,\vec{\jmath} + \sin(i)\,\sin(\omega+\nu)\,\vec{k}\end{aligned}$$

so, the averaging over the fast variable τ_2, is performed according to the following relation

$$\langle Q \rangle = \frac{1}{T}\int_0^T Q\,\mathrm{d}t = \frac{1}{2\pi}\int_0^{2\pi} Q\,\mathrm{d}M = \frac{(1-e^2)^{\frac{3}{2}}}{2\pi}\int_0^{2\pi}\frac{Q\ \mathrm{d}\nu}{(1+e\,\cos\nu)^2}.$$

Rotational Motion

Let us consider the attitude dynamics first. We obtained that the rotational state for a FRT is governed by Eqs. (26-29). We also found that in the time scale of the orbital motion, $\tau_2 = \mathcal{O}(1)$, the plane of rotation remains constant for the asymptotic limit $n/\Omega_\perp \to 0$, which decouples the translational and rotational dynamics. This asymptotic solution, $\dot{\phi}_1 = \dot{\phi}_2 = 0$, which is just valid for the aforementioned time scale, is very often taken for granted for even slower time scales, though this may not necessarily hold true, depending on the ratio $n/\Omega_\perp$. Therefore, one has to be careful and aware of this tacit assumption not to end up with an inadequate modeling when studying the dynamics of FRTs for very large time spans. Probably not to lose the benefits of a decoupled system, the fact is that, to the authors' knowledge, these equations have not been averaged any further than this in the literature, despite the clear implications in their range of validity. As the aim of this article is precisely to reliably study the very long-term dynamics of FRTs, even when it leads to a roto-translational problem, it is necessary to keep on averaging the equations for the attitude dynamics.

Since the only source of torque considered is due to the gravitational interaction of the tether with the planetary satellite, but not with the planet, a single averaging over τ_2 will suffice. At this point, it is very useful to express the dot products on the right-hand side as

$$\begin{aligned}(\vec{u}_G\cdot\vec{v}_1) &= \mathbb{A}\,\cos\nu + \mathbb{B}\,\sin\nu\\ (\vec{u}_G\cdot\vec{v}_2) &= \mathbb{C}\,\cos\nu + \mathbb{D}\,\sin\nu\\ (\vec{u}_G\cdot\vec{v}_3) &= \mathbb{E}\,\cos\nu + \mathbb{F}\,\sin\nu\end{aligned}$$

where the coefficients $\mathbb{A}$ to $\mathbb{D}$ are functions of the orbital elemenents and Tait-Bryan rotation angles. After some algebraic manipulations, these coefficients turn out to be

$$\begin{aligned}\mathbb{A} = &\ [\cos\Omega\,\cos\omega - \cos i\,\sin\Omega\,\sin\omega]\,\cos\phi_2 +\\ &+[\sin\Omega\,\cos\omega + \cos i\,\cos\Omega\,\sin\omega]\,\sin\phi_2\,\sin\phi_1 +\\ &-\sin i\,\sin\omega\,\sin\phi_2\,\cos\phi_1\end{aligned}$$

$$\begin{aligned}\mathbb{B} = &-[\cos\Omega\,\sin\omega + \cos i\,\sin\Omega\,\cos\omega]\,\cos\phi_2 +\\ &-[\sin\Omega\,\sin\omega - \cos i\,\cos\Omega\,\cos\omega]\,\sin\phi_2\,\sin\phi_1 +\\ &-\sin i\,\cos\omega\,\sin\phi_2\,\cos\phi_1\end{aligned}$$

$$\mathbb{C} = \ [\sin\Omega\,\cos\omega + \cos i\,\cos\Omega\,\sin\omega]\,\cos\phi_1\ +\ \sin i\,\sin\omega\,\sin\phi_1$$

$$\mathbb{D} = -[\sin\Omega\,\sin\omega - \cos i\,\cos\Omega\,\cos\omega]\,\cos\phi_1\ +\ \sin i\,\cos\omega\,\sin\phi_1$$

$$\begin{aligned}\mathbb{E} = &\ [\cos\Omega\,\cos\omega - \cos i\,\sin\Omega\,\sin\omega]\,\sin\phi_2 +\\ &-[\sin\Omega\,\cos\omega + \cos i\,\cos\Omega\,\sin\omega]\,\cos\phi_2\,\sin\phi_1 +\\ &+\sin i\,\sin\omega\,\cos\phi_2\,\cos\phi_1\end{aligned}$$

$$\begin{aligned}\mathbb{F} = &-[\cos\Omega\,\sin\omega + \cos i\,\sin\Omega\,\cos\omega]\,\sin\phi_2 +\\ &+[\sin\Omega\,\sin\omega - \cos i\,\cos\Omega\,\cos\omega]\,\cos\phi_2\,\sin\phi_1 +\\ &+\sin i\,\cos\omega\,\cos\phi_2\,\cos\phi_1\end{aligned}$$

This considerably simplifies the averaging process by allowing the right-hand sides of Eqs. (26-29) to be written as

$$\left\langle \frac{1}{r_G^3}(\vec{u}_G \cdot \vec{v}_1)(\vec{u}_G \cdot \vec{v}_3) \right\rangle = \mathbb{A}\,\mathbb{E} \left\langle \frac{\cos^2 \nu}{r_G^3} \right\rangle + \mathbb{B}\,\mathbb{F} \left\langle \frac{\sin^2 \nu}{r_G^3} \right\rangle + (\mathbb{A}\,\mathbb{F} + \mathbb{B}\,\mathbb{E}) \left\langle \frac{\cos\nu\,\sin\nu}{r_G^3} \right\rangle$$

$$\left\langle \frac{1}{r_G^3}(\vec{u}_G \cdot \vec{v}_2)(\vec{u}_G \cdot \vec{v}_3) \right\rangle = \mathbb{C}\,\mathbb{E} \left\langle \frac{\cos^2 \nu}{r_G^3} \right\rangle + \mathbb{D}\,\mathbb{F} \left\langle \frac{\sin^2 \nu}{r_G^3} \right\rangle + (\mathbb{C}\,\mathbb{F} + \mathbb{D}\,\mathbb{E}) \left\langle \frac{\cos\nu\,\sin\nu}{r_G^3} \right\rangle$$

and the resulting averaged terms are easily calculated

$$\left\langle \frac{\cos^2 \nu}{r_G^3} \right\rangle = \frac{1}{2\,a^3\,(1-e^2)^{\frac{3}{2}}} \qquad \left\langle \frac{\sin^2 \nu}{r_G^3} \right\rangle = \frac{1}{2\,a^3\,(1-e^2)^{\frac{3}{2}}} \qquad \left\langle \frac{\cos\nu\,\sin\nu}{r_G^3} \right\rangle = 0$$

Thus, the equations that rule the long-term attitude dynamics of a FRT are the following

$$\frac{\mathrm{d}\phi_1}{\mathrm{d}t} = \frac{n^2}{\Omega_\perp}\frac{3}{4}\,\frac{1}{\cos\phi_2}\,\frac{\mathbb{A}\,\mathbb{E} + \mathbb{B}\,\mathbb{F}}{(1-e^2)^{\frac{3}{2}}} \tag{30}$$

$$\frac{\mathrm{d}\phi_2}{\mathrm{d}t} = \frac{n^2}{\Omega_\perp}\frac{3}{4}\,\frac{\mathbb{C}\,\mathbb{E} + \mathbb{D}\,\mathbb{F}}{(1-e^2)^{\frac{3}{2}}} \tag{31}$$

$$\frac{\mathrm{d}\phi_3}{\mathrm{d}t} = \Omega_\perp - \frac{n^2}{\Omega_\perp}\frac{3}{4}\,\tan\phi_2\,\frac{\mathbb{A}\,\mathbb{E} + \mathbb{B}\,\mathbb{F}}{(1-e^2)^{\frac{3}{2}}} \tag{32}$$

$$\frac{\mathrm{d}\Omega_\perp}{\mathrm{d}t} = 0 \tag{33}$$

Equation (33) indicates that the perturbations considered do not alter, in average, the spinning rate of the FRT, $\Omega_\perp$, which remains constant. Also, Equations (30) and (31) are coupled and independent from ϕ_3. Therefore, we can drop the equations for $\Omega_\perp$ and ϕ_3, since they are irrelevant to describe the attitude of the plane of rotation, and reduce the problem to studying just the evolution of ϕ_1 and ϕ_2.

We can check the validity of these equations upon numerical simulations (see Figure 4) and see how these averaged equations effectively remove from the Tait-Bryan angles the noisy oscillations due to the short-period dynamics, and show just the smooth long-term evolution of the angles

Another interesting observation from Figure 4 arises from the comparison of the averaged equations with varying and non-varying orbital elements (respectively black and green lines), i.e. averaged equations with and without roto-translational coupling, respectively. Their deviation indicates that the time scale in which the orbital elements change and the tether's attitude change might be similar (recall this depends on the ratios $n/\Omega_\perp$ and n_3/n), and if this is the case, the rotational and translational problems have to be integrated simultaneously.

Translational Motion

The translational part of the problem, given by Eqs. (6-11), should be equally averaged. As mentioned before, the disturbing potential, $\mathcal{R}$, has contributions that evolve both in the time scale $\tau_2 = \mathcal{O}(1)$, as in the time scale $\tau_3 = \mathcal{O}(1)$, so a double averaging is required in the fast variables τ_2 and τ_3. However, the disturbing potentials due to the perturbation of the tether, $\mathcal{R}_T$, and the oblanteness of the primary, $\mathcal{R}_{J2}$, solely depend on the orbital motion of the tether, so a single averaging suffices. Hence, averaging equation (23) over τ_2 yields

$$\hat{\mathcal{R}}_T = \frac{\mu\,m\,a_2\,L_T^2}{a^3\,(1-e^2)^{\frac{3}{2}}}\left[\frac{1}{2} - \frac{3}{8}(\mathbb{A}^2 + \mathbb{B}^2 + \mathbb{C}^2 + \mathbb{D}^2)\right] \tag{34}$$

where the hat indicates the averaged value of the disturbing potential. Analogously, averaging Eq. (25) over τ_2 provides

$$\hat{\mathcal{R}}_{J2} = \frac{\mu\,m\,J_2\,R}{a^3\,(1-e^2)^{\frac{3}{2}}}\left[\frac{3}{4}\,\sin^2(i) - \frac{1}{2}\right] \tag{35}$$

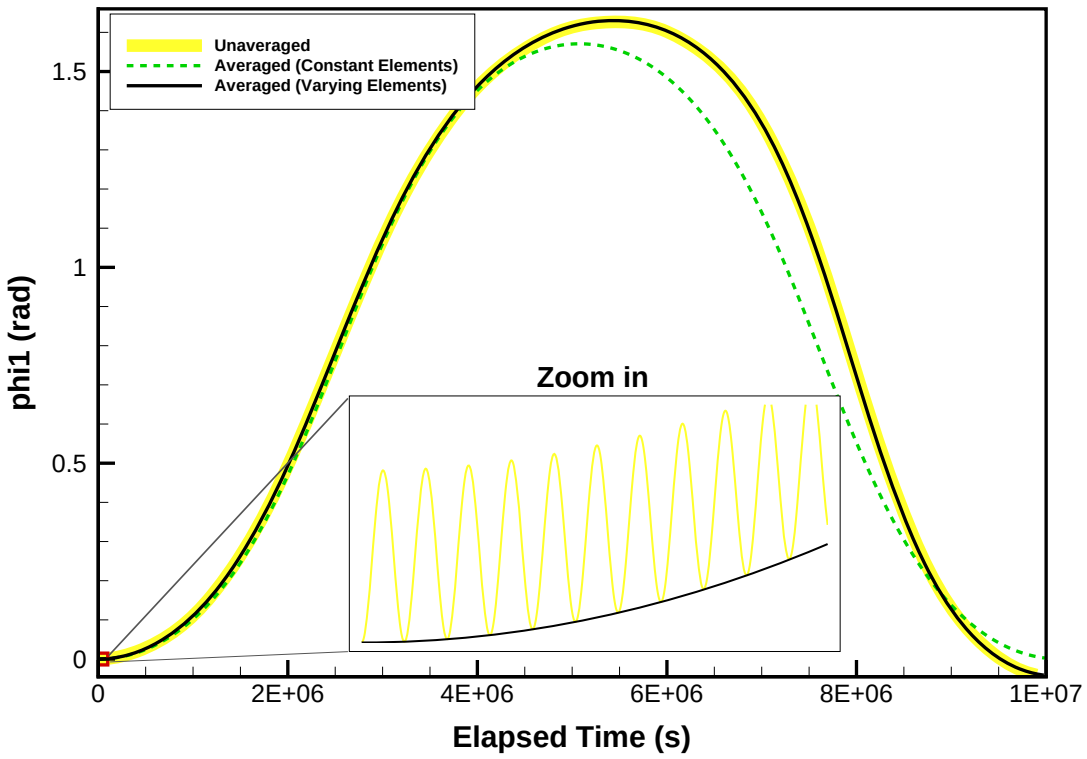

Figure 4: **Evolution of angle Tait-Bryan angle ϕ_1 for an example scenario, as computed with the averaged equations (30-33) and the unaveraged equations (16-19). Two results for the averaged equations are shown, one where the orbital elements have been considered constant (green), and another obtained by integrating the full roto-translational problem in which the orbital elements also vary (black). The unaveraged solution (yellow) was also obtained with varying orbital elements, through numerical simulation.**

The perturbing potential of the third-body, however, does need to be averaged twice, first in over τ_2 and then over τ_3. To perform the first averaging of Eq. (25) over τ_2 we need to make use of the relations

$$\begin{aligned}\langle r_G^2 \rangle &= a^2 \left(1 + \frac{3}{2}\, e^2\right) \\ \langle r_G^2 \, \cos^2 \nu \rangle &= a^2 \left(\frac{1}{2} + 2\, e^2\right) \\ \langle r_G^2 \, \sin^2 \nu \rangle &= a^2 \, \frac{1}{2} \, (1 - e^2)\end{aligned}$$

where it is necessary to switch to the eccentric anomaly, Æ, for these integrals to be solved. Once we take these averaged functions on account, it is straightforward to average the potential to get

$$\langle \tilde{\mathcal{R}}_{3B} \rangle = -\frac{\mu_3 \, m}{\rho^3} \, a^2 \, \frac{3}{4} \left[\mathbb{I}^2 \, (1 + 4\, e^2) + \mathbb{J}^2 \, (1 - e^2) - \left(\frac{2}{3} + e^2\right)\right]$$

with

$$\begin{aligned}\mathbb{I} &= -\cos(\Omega - \Theta) \, \cos\omega + \sin(\Omega - \Theta) \, \cos i \, \sin\omega \\ \mathbb{J} &= +\cos(\Omega - \Theta) \, \sin\omega + \sin(\Omega - \Theta) \, \cos i \, \cos\omega\end{aligned}$$

where the angle Θ stands for the true anomaly of the satellite in its orbit around the planet. This motion is, by the definition of our pseudo-inertial reference frame, contained in the x_1y_1 plane. For the last averaging, $\tau_3 = \Theta$ is the fast variable of the motion. At this point, it makes things easier to suppose the satellite follows a circular orbit around the planet, such that the anomaly Θ varies linearly with time, and averaging reduces to integrating in Θ over a period. Note that this assumption is indeed realistic, as most planetary satellites in the Solar System have nearly circular orbits. Thus, the final averaged disturbing potential of the third body would be

$$\hat{\mathcal{R}}_{3B} = \langle\langle\tilde{\mathcal{R}}_{3B}\rangle\rangle = -\frac{\mu_3\, m}{\rho^3}\, a^2\, \frac{3}{4}\, \left[\langle\mathbb{I}^2\rangle\,(1+4\,e^2) + \langle\mathbb{J}^2\rangle\,(1-e^2) - \left(\frac{2}{3}+e^2\right)\right] \tag{36}$$

with

$$\langle\mathbb{I}^2\rangle = \frac{1}{2}(\cos^2 i + \cos^2\omega - \cos^2 i\,\cos^2\omega)$$
$$\langle\mathbb{J}^2\rangle = \frac{1}{2}(\sin^2\omega + \cos^2 i\,\cos^2\omega)$$

Obviously, the total disturbing potential that needs to be used in the Lagrange planetary equations (6-11) is the sum of Equations (34-36), i.e.

$$\hat{\mathcal{R}} = \hat{\mathcal{R}}_T + \hat{\mathcal{R}}_{J2} + \hat{\mathcal{R}}_{3B} \tag{37}$$

and now the orbital elements $\{a, e, i, \omega, \Omega, M\}$ are not the instantaneous osculating values, but rather the *mean* values of the orbit of the FRT.

LONG-TERM DYNAMICS

In the previous section we derived the equations that describe the motion of a FRT around a planetary satellite in the long-term. The whole set of equations comprises 1) the Lagrange planetary equations, Eqs. (34-36), along with the averaged disturbing potential, $\hat{\mathcal{R}}$, from Eq. (37), to solve the translational motion, and 2) Equations (30-31) to account for the rotational motion. In the general case, the translational and rotational motions of a FRT are coupled, so the whole set of equations must be integrated simultaneously. Therefore, one wonders if, for certain values of $n/\Omega_\perp$ and n_3/n, there is any time scale for which rotational and translational motions can be decoupled. In the previous section we saw that $\tau \ll \tau_3 \ll \tau_2 \ll \tau_1$, where $\tau = \mathcal{O}(1)$ is the time scale where the orbital elements vary. Attending at the Lagrange equations, the orbital elements will vary at a rate given by the perturbing potential, and the considered perturbing forces and their time scales. In our model, the perturbation with the slowest time scale, and hence the most stringent perturbation in this sense, is the third-body perturbation of the planet, which takes place in the time scale $\tau_3 = \mathcal{O}(1)$. Therefore, we can conclude that characteristic time where orbital elements suffer variations is $T = n/n_3^2$, so the non-dimensional time τ takes the form

$$\tau = t/T = \frac{n_3^2}{n}\, t$$

However, if we pay attention at Equations (30-31) we realize that the attitude dynamics evolves in a different time scale, which allows us to define the characteristic time $T_R = \Omega_\perp/n^2$. Thus, we can define the new non-dimensional time, τ_R, as

$$\tau_R = t/T_R = \frac{n^2}{\Omega_\perp}\, t$$

We can guarantee that $T_R \gg T_2$, but in principle nothing can be said whether T_R is less of greater than T_3, as this will depend on the values n_3 and $\Omega_\perp$. Consequently, both time scales related to T and T_R, are slow compared to T_2. Actually, they are in principle comparable, i.e. $T \sim T_R$, and that is why the problem is roto-translationally coupled, but this is not necessarily always so. The time T is basically imposed by the scenario, i.e. given a planetary satellite n and n_3 are fixed, then so is T. The rotation of the tether, however, is a design parameter, so in principle we should have the freedom to choose a value for $\Omega_\perp$, which indirectly

fixes the time scale where the attitude of the tether plane of rotation will evolve, T_R. Therefore, depending on the value of $\Omega_\perp$, it may happen that $T_R \gg T \gg T_3$, or $T \gg T_R \gg T_3$ or even $T \gg T_3 \gg T_R$, so it is necessary to have some means for comparing all these three time scales with each other. This way, if the time scale $\tau_R = \mathcal{O}(1)$ is much faster or slower than the time scale $\tau = \mathcal{O}(1)$, we should be able to decouple the dynamics. This is easily concluded if we define a non-dimensional parameter, χ, as the ratio

$$\chi = \frac{\tau_R}{\tau} = \frac{T}{T_R} = \left(\frac{n}{\Omega_\perp}\right)\left(\frac{n}{n_3}\right)^2$$

Then, if $\chi \ll 1$, the time scale in which the plane of the FRT evolves is much slower than the time scale where the orbital elements vary. Therefore, the attitude of the tether may be considered *frozen* or *quasi-stationary* in the study of the orbital motion. Inversely, if $\chi \gg 1$, then the change in the attitude dynamics is so much faster that the orbital elements may be seen as frozen for the study or the rotational problem. If $\chi \sim 1$, the problem remains coupled. In the following, we will analyze a little bit more in detail each of these two limit cases where the decoupling is legit.

Extended Frozen Orbits

In the case $\chi \ll 1$, the system decouples and we may study the translational motion assuming the mean values of ϕ_1 and ϕ_2 keep their initial value. Even so, the study of Equations (34-36) remains truly difficult due to the complexity of the disturbing potential $\hat{\mathcal{R}}$, so in order to get some insight about the dynamics it is only reasonable to try to find some sort of simplifying assumption that reduces this complexity. A convenient simplification is achieved by choosing $\phi_1 = \phi_2 = 0$, i.e. setting the plane of rotation of the tether parallel to the equator of the primary. Under this assumption, the equations of motion drastically simplify to

$$\frac{\mathrm{d}a}{\mathrm{d}t} = 0 \tag{38}$$

$$\frac{\mathrm{d}e}{\mathrm{d}t} = \frac{\mu_3}{\rho^3}\,\frac{e\sqrt{1-e^2}}{n}\,\frac{15}{8}\,\sin(2\,\omega)\,\sin^2(i) \tag{39}$$

$$\frac{\mathrm{d}i}{\mathrm{d}t} = -\frac{\mu_3}{\rho^3}\,\frac{e^2}{n\sqrt{1-e^2}}\,\frac{15}{16}\,\sin(2\,\omega)\,\sin(2\,i) \tag{40}$$

$$\begin{aligned}\frac{\mathrm{d}\omega}{\mathrm{d}t} = {} & \frac{\mu}{n\,a^5\,(1-e^2)^2}\,\frac{3}{8}\left(5\,\cos^2 i - 1\right)\left[a_2\,L_T^2 + 2\,J_2\,R^2\right] + \\ & + \frac{\mu_3}{\rho^3}\,\frac{\sqrt{1-e^2}}{n}\,\frac{3}{4}\left[4\,\cos^2 i + 5\,\cos^2\omega - 5\,\cos^2 i\,\cos^2\omega - 3\right] + \\ & + \frac{\mu_3}{\rho^3}\,\frac{\cos^2 i}{n\sqrt{1-e^2}}\,\frac{3}{4}\left[1 + (5\,\sin^2\omega - 1)\,e^2\right]\end{aligned} \tag{41}$$

$$\begin{aligned}\frac{\mathrm{d}\Omega}{\mathrm{d}t} = {} & \frac{-\cos i}{n\,a^2\,\sqrt{1-e^2}}\,\frac{3}{4}\cdot \\ & \cdot\left[\frac{\mu}{a^3\,(1-e^2)^{\frac{3}{2}}}\,\left(a_2\,L_T^2 + 2\,J_2\,R^2\right) + \frac{\mu_3}{\rho^3}\,a^2\,\left(1 + (5\,\sin^2\omega - 1)\,e^2\right)\right]\end{aligned} \tag{42}$$

This set of equations is similar to those obtained by other authors[9,10,11,12] who success to include the gravity perturbation due to J_2, but the novelty of our formulation is that Eqs (38-42) additionally include the mechanical perturbation due to the FRT.

A very interesting application of these equations is that they may be used to compute frozen orbits around planetary satellites. Frozen orbits are obtained as the stationary solutions of Equations (38-42), where the variation of the mean anomaly, M, is irrelevant as it does not change the shape nor the orientation of the orbit, therefore is not presented here. This issue was already addressed in References 5 and 6, where the latter reference shows a more elaborated computation of frozen orbits with the inclusion of an arbitrary number of zonal harmonics in the calculations. Note that we may include further harmonics in our analysis by replacing $\hat{\mathcal{R}}_{J2}$, from Eq. (35), by the following averaged potential

$$\hat{\mathcal{R}}_{Jn} = -\frac{\mu}{r_G} \sum_{n\geq 2} \left(\frac{R}{r_G}\right)^n J_n \sum_{p=0}^{n} F_{n,0,p}(i)\, G_{n,p,(2p-n)}(e) \begin{cases} \cos[(n-2p)\,\omega] & \text{if } (l-2p) \text{ is even} \\ \sin[(n-2p)\,\omega] & \text{if } (l-2p) \text{ is odd} \end{cases}$$

where $F(i)$ and $G(e)$ are Kaula's inclination and eccentricity functions, respectively.[13]

The most relevant result obtainable from these equations is that a FRT rotating in a plane parallel to the equator actually increases the regression of nodes, since its contribution directly sums to that of the primary's oblateness. This fact has beneficial effects in stabilizing the orbital motion, an more particularly in lowering the eccentricity of frozen orbits, by the simple expedient of lengthening an inert rotating tether.[6]

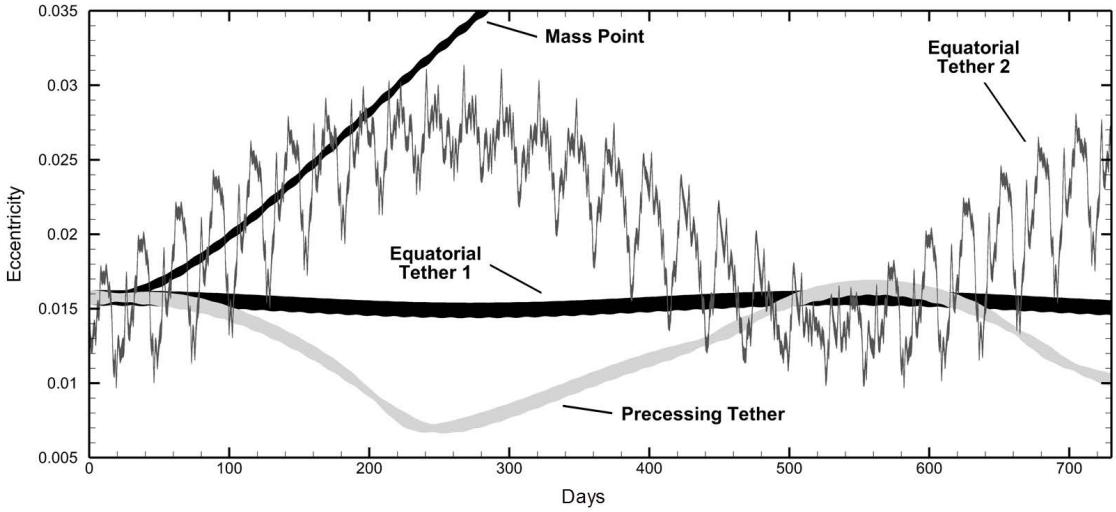

Figure 5: Eccentricity evolution of a 50 km FRT ($\Omega_\perp = 0.1$ rad/s) for a low-altitude ($a = 1838$ km), high inclination ($i = 81°$) lunar orbit, using different dynamical models, beginning at epoch J2000.0. **Mass Point** considers the tether as being a mass point. **Equatorial Tether 1** is a tether such that the plane of rotation is forced to remain parallel to the equator and 150 zonal harmonics are included. **Equatorial Tether 2** considers instead a 50x50 subset of spherical harmonics, including tesseral and sectorial harmonics. **Precessing Tether** is the same case as 'Equatorial Tether 1', but the tether plane of rotation evolves freely according to the coupled orbital-rotational dynamics. Results taken from Reference 6

Nevertheless, these *extended* frozen orbits with lower eccentricity exist only for as long as our system remains uncoupled, i.e. they do not last long if $\chi \sim 1$ since the attitude coupling changes the orientation of the FRT's plane of rotation, which varies the orbital perturbations such that they do not satisfy the frozen orbit solution. In order to illustrate this phenomenon, Figure 5 shows the temporal variation of the eccentricity for a frozen low lunar orbit. All solutions represented in Figure 5 were numerically computed with non-averaged equations, but under different force models and assumptions on the attitude of the FRT's plane of rotation. More particularly, the solution labeled as 'Equatorial Tether 1' was started with initial conditions that correspond to a frozen orbit calculated under the perturbations of 150 zonal harmonics, and propagated forward assuming the plane of rotation or the FRT remains always parallel to the equator, namely $\phi_1 = \phi_2 = 0$. Numerically, we observe that the orbit, on average, preserves the initial eccentricity. However, if we allow the plane of rotation to freely evolve according to the roto-translational motion (solution labeled as

'Precessing Tether'), then ϕ_1 and ϕ_2 vary, producing a drift in the eccentricity and killing the frozen orbit. This is easily understood if we compute the value of the parameter χ in this scenario:

$$\begin{aligned}\Omega_\perp &= 0.1 \text{ rad/s}\\ n &= 8.886\cdot 10^{-4} \text{ rad/s}\\ n_3 &= 2.649\cdot 10^{-6} \text{ rad/s}\\ \chi &\simeq 1000\end{aligned}$$

and as we expected, the value of χ confirms that the coupling was important enough to prevent the frozen orbit from lasting too long.

Precession of the FRT

The rotational motion is governed by Equations (30) and (31), that may be rewritten as a function of the non-dimensional time τ_R, which highlights the real time scale where the plane of rotation evolves

$$\begin{aligned}\frac{\mathrm{d}\phi_1}{\mathrm{d}\tau_R} &= \frac{3}{4}\frac{1}{\cos\phi_2}\frac{\mathbb{A}\,\mathbb{E}+\mathbb{B}\,\mathbb{F}}{(1-e^2)^{\frac{3}{2}}}\\ \frac{\mathrm{d}\phi_2}{\mathrm{d}\tau_R} &= \frac{3}{4}\frac{\mathbb{C}\,\mathbb{E}+\mathbb{D}\,\mathbb{F}}{(1-e^2)^{\frac{3}{2}}}\end{aligned}$$

In the case $\chi \gg 1$, these equations also decouple from the translational problem, assuming that the mean orbital elements maintain their initial value. Still, the evolution of ϕ_1 and ϕ_2 depends on the values of these orbital elements through the functions $\mathbb{A}$ to $\mathbb{F}$, making their general solution non trivial. Therefore, we may try to use some simplifying assumptions in order to get some insight in the problem.

A good first try is to consider an equatorial orbit, namely $i = 0$. Doing so equations (30) and (31) drastically reduce to

$$\begin{aligned}\frac{\mathrm{d}\phi_1}{\mathrm{d}\tau_2} &= \frac{n}{\Omega_\perp}\frac{3}{4}\sin\phi_2\,\cos^2\phi_1\\ \frac{\mathrm{d}\phi_2}{\mathrm{d}\tau_2} &= -\frac{n}{\Omega_\perp}\frac{3}{4}\cos\phi_2\,\cos\phi_1\,\sin\phi_1\end{aligned}$$

where any dependency with the orbital elements has been removed. From this system one can easily obtain a first integral of the motion, simply dividing both equations, which yields

$$\frac{\mathrm{d}\phi_1}{\mathrm{d}\phi_2} = -\frac{\tan\phi_2}{\tan\phi_1} \tag{43}$$

and the differential equation may be solved to provide

$$\cos\phi_1\,\cos\phi_2 = \cos\Phi \tag{44}$$

where Φ is a constant that can be determined from the initial values of ϕ_1 and ϕ_2. Φ is easily identifiable as the angle between the tether's angular momentum vector, $\vec{H}_G$, and the direction perpendicular to the orbital plane, $\vec{k}$. This reveals that given a certain initial position of the rotation plane (given a value to Φ), the angles ϕ_1 and ϕ_2 will evolve satisfying Eq. (44). We get a visual description of this by plotting the direction field of the differential equation (43), shown in Figure 6, which is the phase space of ϕ_1 and ϕ_2. The evolution of the dynamics is such that angles ϕ_1 and ϕ_2 follow closed curves in the phase space, moving clockwise.

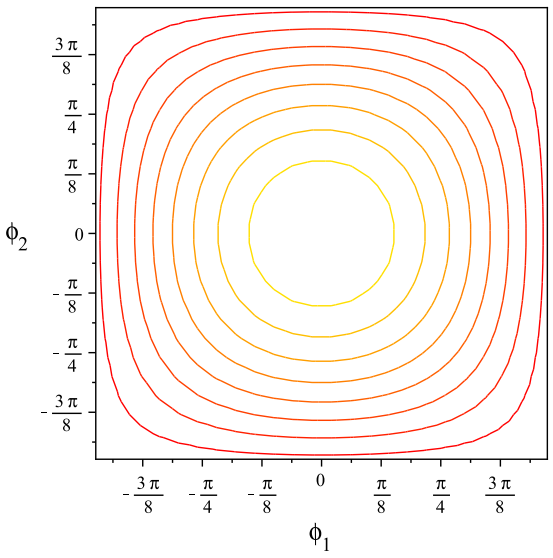

Figure 6: **Phase space of ϕ_1 and ϕ_2 for different values of Φ, under the assumption $i = 0$.**

We shall also note that the variations of ϕ_1 and ϕ_2 are stable in the sense that, given an initial state, the FRT's plane of rotation will evolve in a way that its angular momentum vector will preserve the very same angle Φ with respect to the polar axis, z_1. In other words, the FRT's plane of rotation preceeds around z_1. Also, $\phi_1 = \phi_2 = 0$ is an equilibrium point that kills the precession, so the plane of rotation remains in the equatorial plane. On the contrary, $\phi_1 = \pm\frac{\pi}{2}$ turns out to be unstable, meaning that if the angular momentum vector is ever contained in the equatorial plane, then the FRT's attitude would drift away.

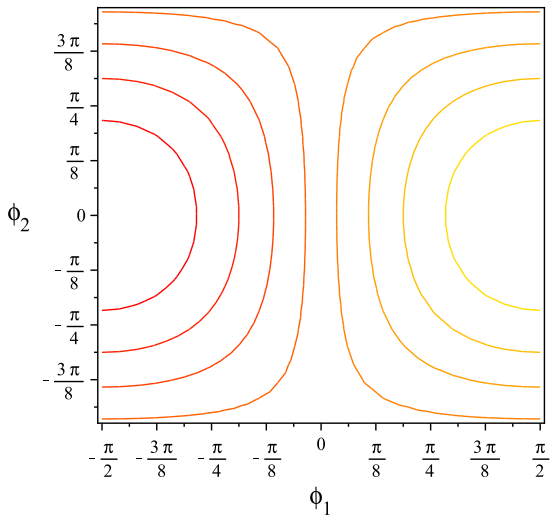

Figure 7: **Phase space of ϕ_1 and ϕ_2 for different values of Φ, under the assumption $i = \pi/2$.**

Another significant case is found when the orbit is polar instead, namely $i = \pi/2$. In this case, Equations (30) and (31) simplify too, but a dependency with Ω remains. This happens because of the orientation of the inertial unit vectors $\{\vec{i}_1, \vec{j}_1, \vec{k}_1\}$ to which Tait-Bryan angles are referenced, and simply choosing $\vec{i}_1$ such that it is aligned with the orbital line of nodes would eliminate this dependence. Hence, in order to simplify the equations as much as possible, we simply choose to particularize for $\Omega = 0$, without any loss of generality, which reduces the equations to

$$\frac{\mathrm{d}\phi_1}{\mathrm{d}\tau} = \frac{n}{\Omega_\perp}\frac{3}{4}\sin\phi_2\,\sin^2\phi_1$$
$$\frac{\mathrm{d}\phi_2}{\mathrm{d}\tau} = \frac{n}{\Omega_\perp}\frac{3}{4}\cos\phi_2\,\cos\phi_1\,\sin\phi_1$$

Again, dividing both equation leads to

$$\frac{\mathrm{d}\phi_1}{\mathrm{d}\phi_2} = \tan\phi_1\,\tan\phi_2 \tag{45}$$

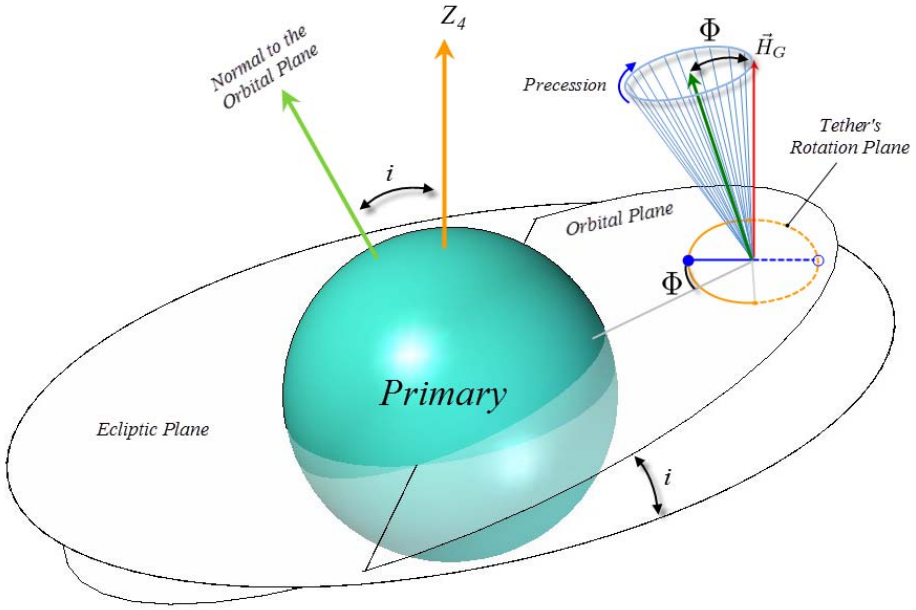

Figure 8: **Scheme illustrating the precession of the tether's plane of rotation**

which can be solved to provide a first integral of the motion

$$\sin\phi_1 \, \cos\phi_2 = \cos\Phi \tag{46}$$

where Φ is a constant that can be determined from the initial values of ϕ_1 and ϕ_2, and again, Φ turns out to be the angle between the tether's angular momentum vector and the direction perpendicular to the orbital plane, in this time a polar orbit.

We can observe great similarities with the case of an equatorial orbits. Again, a precession of the angular momentum vector takes place around the direction perpendicular to the orbital plane, which is stable and preserves the value of Φ. Also, there is a equilibrium point for $\Phi_2 = 0$ that kills the precession, whereas the rotation becomes unstable when the angular momentum vector is contained in the equatorial plane. The phase space (see Figure 7) also preserves the same structure as in Figure 6, except for a shift in the horizontal axis, ϕ_1, that coincides with the value of the orbital inclination.

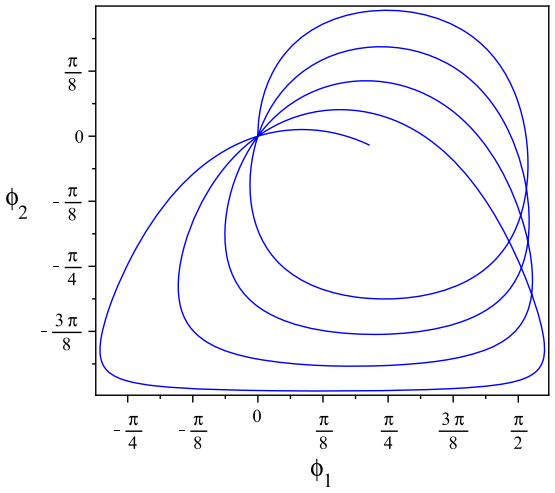

Figure 9: **Phase space of ϕ_1 and ϕ_2 for the simulation as in Figure 4, with $\chi \simeq 57$**

This fact suggests that this shift could actually happen for any arbitrary orbital inclination and the shift be exactly the inclination, i. Though we could not mathematically prove this directly from the Equations (30-31), we succeeded to confirm this fact numerically. Note that this is actually very reasonable, as in fact, a FRT around a primary may be seen, from a mechanical point of view, as essentially the very same problem as the Earth orbiting around the Sun, where the Earth rotation axis is subject to a precession.

Hence, we can conclude that a precession of the FRT's angular momentum vector occurs around the direction perpendicular to the orbital plane, as sketched in Figure 8. The rate at which the angular momentum precesses is a function of the ratio $n^2/\Omega_\perp$ and the precession angle, Φ, is imposed by the initial conditions $\phi_1(0)$, $\phi_2(0)$ and the orbital inclination $i(0)$. Φ remains constant for as long as the orbital elements can be considered quasi-stationary, i.e. for $\chi \gg 1$. For instance, we have already seen in Figure 4 an example where $\chi \simeq 57$, and the variation in the orbital elements has consequently a visible impact when studying the dynamics of the plane of rotation. In such cases where the problem accepts no decoupling, the variables ϕ_1 and ϕ_2 do not form closed orbits in their phase space (Figures 6 and 7), but describe instead open trajectories as shown in Figure 9.

CONCLUSIONS

In this article we have derived a formulation for the coupled roto-translational motion of a fast rotating tether around planetary satellites, that describes the long-term dynamics. We have identified that the motion takes place in several different time scales, associated the following characteristic times

T_1**:** the characteristic time of the self-rotation of spinning of the tether

T_2**:** the orbital motion of the tether around the satellite

T_3**:** the orbital motion of the satellite around the planet, which rules the third-body perturbation

T**:** a slower time scale where the tether's orbital elements vary

T_R**:** another slow time scale where the plane of rotation of the fast-rotating tether evolves

Under the assumptions that $T \gg T_3 \gg T_2 \gg T_1$, and $T_R \gg T_2$, these equations have been derived by successively using the averaging technique in the three fastest time scales of the problem, in order to obtain final expressions that govern the variation of the mean orbital elements of the tether, and the average attitude of its plane of rotation.

Though in principle the translational and rotational motions are coupled, attending at the averaged set of equations, we have noted that, depending on the spinning rate of the tether, the long-term evolution of the its attitude does not necessarily take place in the same time scale as the orbital motion. Therefore, the problem admits to be decoupled in some cases:

If $T \ll T_R$, then the attitude of the tether plane of rotation may be taken as quasi-stationary, and the equations for the translational motion may be used to compute lower eccentricity frozen orbits, thanks to the beneficial perturbing effect of the rotating tether. The lifetime of these extended frozen orbits is limited by the time scale that rules the attitude dynamics, and can be increased with a higher spinning rate of the tether.

If $T \gg T_R$, then the mean orbital elements of the tether may be taken as quasi-stationary in the study of the attitude dynamics of its plane of rotation. In this regime, the angular momentum vector of the tether precesses around the normal to the orbital plane.

ACKNOWLEDGMENT

This work was carried out in the framework of the research project entitled **Dynamic Simulation of Complex Space Systems** (AYA2010-18796) supported by the Spanish Ministry of Economy and Competitiveness. Authors thank the Spanish Gov. for its support.

We would also like to thank the Techical University of Madrid (UPM) for supporting Hodei Urrutxua in the development of his Ph.D. Thesis under their graduate scholarship program.

REFERENCES

[1] M. L. Cosmo and E. C. Lorenzini, "Tethers In Space Handbook," tech. rep., Smithsonian Astrophysical Observatory, December 1997. Third Edition.
[2] J. A. Carroll, "Tether applications in space transportation," *Acta Astronautica*, Vol. 13, No. 4, 1986, pp. 165 – 174, http://dx.doi.org/10.1016/0094-5765(86)90061-5.
[3] J. Peláez and M. Sanjurjo, "Generator Regime of Self-Balanced Electrodynamic Bare Tethers," *Journal of Spacecraft and Rockets*, Vol. 43, November-December 2006, pp. 1359–1369.
[4] J. Peláez, M. Sanjurjo, F. R. Lucas, M. Lara, E. C. Lorenzini, D. Curreli, and D. J. Scheeres, "Dynamics and Stability of Tethered Satellites at Lagrangian Points," Ariadna Study 07/4201, European Space Agency, 2007.
[5] H. Urrutxua, J. Peláez, and M. Lara, "Frozen Orbits for Scientific Missions Using Rotating Tethers," *Advances in the Astronautical Sciences*, Vol. 143, Charleston, SC, USA, 22nd AAS/AIAA Space Flight Mechanics Meeting, 2012, pp. 2475–2490.
[6] M. Lara, J. Pelez, and H. Urrutxua, "Modifying the atlas of low lunar orbits using inert tethers," *Acta Astronautica*, Vol. 79, No. 0, 2012, pp. 52 – 60, 10.1016/j.actaastro.2012.04.026.
[7] H. Urrutxua, "Use of Rotating Space Tethers in the Exploration of Celestial Bodies," engineering thesis, Technical University of Madrid (UPM), October 2010.
[8] H. Urrutxua, J. Peláez, and M. Lara, "Gravitational Actions upon a Tether in a Non-Uniform Gravity Field with Arbitrary Number of Zonal Harmonics," *24th AAS/AIAA Space Flight Mechanics Meeting*, No. AAS 14-082, Santa Fe, NM, USA, 2014.
[9] K. W. Meyer, J. J. Buglia, and P. N. Desai, "Lifetimes of Lunar Satellite Orbits," Technical Paper 3394, NASA, March 1994.
[10] M. E. Paskowitz and D. J. Scheeres, "Orbit Mechanics About Planetary Satellites - Dynamics of Planetary Satellite Orbiters," *American Astronautical Society*, Vol. 224, 2004, pp. 1–17.
[11] M. Paskowitz Possner and D. J. Scheeres, "Control of Science Orbits About Planetary Satellites," *Journal of Guidance, Control, and Dynamics*, Vol. 32, Jan. 2009, pp. 223–231, 10.2514/1.36220.
[12] M. Lara and J. F. Palacián, "Hill Problem Analytical Theory to the Order Four: Application to the Computation of Frozen Orbits around Planetary Satellites," *Mathematical Problems in Engineering*, Vol. 2009, 2009, pp. 1–19, 10.1155/2009/753653.
[13] W. M. Kaula, *Theory of Satellite Geodesy. Applications of Satellites to Geodesy*. Earth Sciences, Dover Publications, first ed., 2000.